Structural Engineering and Mechanics, *Vol. 56, No. 6 (2015) 1021-1040*
DOI: http://dx.doi.org/10.12989/sem.2015.56.6.1021

Aerodynamic loads and aeroelastic responses of large wind turbine tower-blade coupled structure in yaw condition

S.T. Ke[*1], T.G. Wang[1a], Y.J. Ge[2b] and Y. Tamura[3c]

[1]*Jiangsu Key Laboratory of Hi-Tech Research for Wind Turbine Design, Nanjing University of Aeronautics and Astronautics, Yudao Road 29, Nanjing 210016, China*
[2]*State Key Laboratory for Disaster Reduction in Civil Engineering, Tongji University, Siping Road 1239, Shanghai 200092, China*
[3]*Center of Wind Engineering Research, Tokyo Polytechnic University, 1583 Iiyama, Atsugi, Kanagawa 243-0297, Japan*

(Received August 17, 2014, Revised November 13, 2015, Accepted November 24, 2015)

Abstract. An effective method to calculate aerodynamic loads and aeroelastic responses of large wind turbine tower-blade coupled structures in yaw condition is proposed. By a case study on a 5 MW large wind turbine, the finite element model of the wind turbine tower-blade coupled structure is established to obtain the modal information. The harmonic superposition method and modified blade-element momentum theory are used to calculate aerodynamic loads in yaw condition, in which the wind shear, tower shadow, tower-blade modal and aerodynamic interactions, and rotational effects are fully taken into account. The mode superposition method is used to calculate kinetic equation of wind turbine tower-blade coupled structure in time domain. The induced velocity and dynamic loads are updated through iterative loop, and the aeroelastic responses of large wind turbine tower-blade coupled system are then obtained. For completeness, the yaw effect and aeroelastic effect on aerodynamic loads and wind-induced responses are discussed in detail based on the calculating results.

Keywords: wind turbine tower-blade coupled structure; aerodynamic loads; aeroelastic effect; yaw effect; parameter analysis

1. Introduction

Wind turbines operate at all times in an extremely complex and unsteady flow, and aerodynamic forces acting on the blades vary consistently. The main factors which make a contribution to the unsteady aerodynamic forces on the blades include yawed flow, wind shear, atmospheric turbulence, tower shadow, and structural deformation, etc. The large wind turbine systems including tower and wind blades are typical wind sensitive structures (Agarwal and Manuel 2009, Karimirad *et al.* 2011, Barlas and Van 2009), and therefore the unsteady erodynamic

*Corresponding author, Associate Professor, E-mail: keshitang@163.com
[a]Professor, E-mail: tgwang@nuaa.edu.cn
[b]Professor, E-mail: yaojunge@tongji.edu.cn
[c]Professor, E-mail: yukio@arch.t-kougei.ac.jp

Copyright © 2015 Techno-Press, Ltd.
http://www.techno-press.org/?journal=sem&subpage=8 ISSN: 1225-4568 (Print), 1598-6217 (Online)

loads and structural wind effects are crucial for wind-resistant design of wind turbines. In recent years the blades of the new generation super-large wind turbine systems are much longer than ordinary blades, and the blades diameter is up to a order of hundred meters (Bazeos *et al.* 2002). The aeroelastic effect of the large wind turbine structure is much severer. Furthermore, due to the continuous variation of wind directions and high turbulence characteristics, the wind blades could not mainly keep parallel with wind direction. In this case, the yaw condition will always happens in operation state, and the induced velocity would change in azimuth angle and radial direction, which results in the redistribution of aerodynamic loads on blades and aeroelastic instability of tower.

In latest studies on the aeroelastic responses of large wind turbine system in yaw condition, the twisting vibration of the wind turbine tower in yaw condition was investigated, and the corresponding vibration-reduced measures were given by Jeong and Kim (2013). The aerodynamic responses of blades in yaw condition were discussed, which considers the centrifugal force effect and aeroelasticity effect on dynamic responses (Liao 2009, Shen *et al.* 2011). The modified coupled solution model of blade was proposed by Corson *et al*. (2012), and the calculating model of induced factors for blades considering yaw effect was also proposed. The dynamic stall prediction model for wind turbine blades in yaw condition was established, and the basic principles and characteristics of dynamic stall model caused by yaw effect were discussed (Jiménez *et al.* 2010). By a case study on a new-generation 5MW ultra large wind turbine system, The harmonic superposition and modified blade-element momentum theory are used to predict the aerodynamic loads with the consideration of tower-blade aerodynamic and model interaction, and modification of steady wind (Ke *et al.* 2014). It should be noted that the existing studies were mostly suitable for the wind blades, and the modification of steady wind, aeroelastic effect and yaw effect of the wind turbine tower-blade coupled structure were neglected. Furthermore, with the size increase of super-large wind turbine system, the tower deformation under stochastic wind would be more obvious, and the aeroelastic problem induced by blade and tower deformation would affect wind-induced responses of wind turbine system in yaw condition. In view of the above studies, the accurate prediction method of aerodynamic loads and aeroelastic responses of large wind turbine tower-blade coupled structure in yaw condition is very significant to enhance structural wind resistant safety.

In this paper the aerodynamic loads of large wind turbine tower-blade coupled structure are calculated based on harmonic superposition method and modified blade element momentum theory, in which the yaw angle, wind shear, tower shadow, tower-blade dynamic and modal interaction are fully taken into account. A tower-blade coupled model for a 5 MW large wind turbine is established with finite element method. The kinetic equation of wind turbine tower-blade coupled structure is then solved using mode superposition method, in which the induced velocity and dynamic loads are updated through iterative loop. Finally, the aeroelastic response of large wind turbine tower-blade coupled structure under different yaw angles is discussed in detail.

2. Aerodynamic loads calculation

The fluctuating wind field around the wind turbine system consists of two parts, the fluctuating flow over the tower and the fluctuating flow over the blade. The wind fields of the tower and wind blades interacts each other when the wind turbine is operating, and the wind blades in the wind direction have significant influence on the tower. Importantly, the blade flow field is influenced by

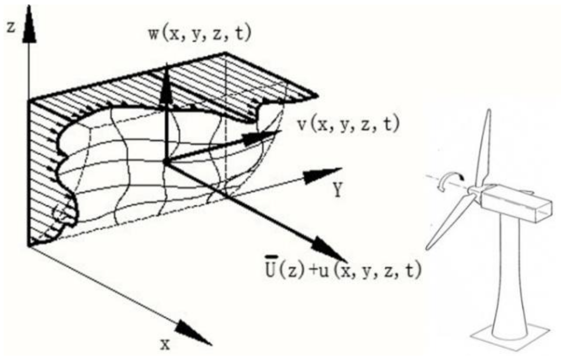

Fig. 1 The wind field model coordinate system of the wind turbine structure

its own rotational effect and interferential effect from the tower. Owing to the inverted cone structure of the tower, the stiffness of each direction is identical. Moreover, the rotor is always regulated to be aligned with the wind direction, which leads to less influence on the lateral and vertical wind field of the wind turbine tower-blade system. The aeroloads on both the blade and the tower mainly result from the fluctuating wind energy along the wind direction. Therefore, the numerical simulation of the fluctuating wind speed along the wind direction is carried out in this paper.

The wind speed model of wind turbine system is composed of steady wind and fluctuating wind, the former is caused by the overall atmosphere movement, and its direction is only horizontal downwind, and the latter is local turbulent motion, which has downwind, crosswind and vertical directions. The wind field model coordinate system of the wind turbine is showed in Fig. 1.

2.1 Modification of steady wind

The steady wind is influenced by the wind shear, tower shadow, wake effect from upstream wind turbines, hence the modification of steady wind should be necessary in aerodynamic loads calculation. The exponential model for wind shear, the undercurrent model for tower shadow effect and eddy viscosity model for wake effect from upstream wind turbine are used to modify the steady wind model (Burton *et al.* 2001).

The wind shear effect is the variation of wind speed with height, the main models include exponential model and logarithmic model. Considering the practical applicability and precision, the power model is used, whose calculating formula is as follows

$$V(h) = V(h_0)(\frac{h}{h_0})^{\alpha} \tag{1}$$

where $V(h)$, $V(h_0)$ represent the average wind speed at height of h and h_0 meters respectively; α is the power law, its value range is 0.1~0.25, which could be set as zero when without considering wind shear effect; h_0 is the hub height.

The tower shadow effect caused by the tower obviously amplify the steady wind speed of blades, there are three revised methods: the undercurrent model for downstream tower, the empirical model for upstream tower, and the combined model. The upstream model are mostly designed in existing wind turbines, which can avoid the additional noise and exciting force caused by the tower, herein the undercurrent model is adopt (Burton *et al.* 2001).

$$V(y,z) = AV_0 \tag{2}$$

$$A = 1 + (\frac{D}{2})^2 \frac{(y^2 - z^2)}{(y^2 + z^2)^2}, D = F \bullet D_T \tag{3}$$

In the formula, D_T is the tower top diameter, F is the correction factor of tower diameter; z is the downwind distance between calculating point and tower center; y is the crosswind distance between calculating point and tower center.

The wind turbines are always constructed as groups form in wind farm, therefore a single wind turbine would be in wake flow of upstream wind turbine, which makes the wake effect significant for the wind field simulation. Herein the eddy viscosity model is adopted to correct the additional turbulence influence induced by wake flow effect, whose calculating formula is as following

$$V = V_0(1 - \Delta e^{-\frac{r^2}{2w^2}}) \tag{4}$$

where r is the distance between local speed and wake center; w is wake width; V_0 is undisturbed average wind speed; Δ is velocity deficit.

2.2 Incoming fluctuating wind simulation

The time series of incoming wind velocity for the tower and the wind blades are both simulated through a harmony superposition method proposed by Shinozuka (Shinozuka and Seya 1990, Kareem 2008), and the method has been used for numerical simulation of stationary random process. Owing to the coherence in three directions of wind blades and towers, the Davenport correlation coefficient (Davenport 1995) is used for calculation of the correlation between the wind blades and the tower.

$$C_{ij} = \exp\left[-\frac{\omega\sqrt{C_x(x_i - x_j)^2 + C_y(y_i - y_j)^2 + C_z(z_i - z_j)^2}}{2\pi v(H)}\right] \tag{5}$$

In the formula, C_x, C_y, C_z are the transverse, downwind, vertical attenuation coefficient of any two points on the wind blades and the tower, respectively; ω is the fluctuating wind frequency; $v(H)$ is the average wind speed at height H.

In this paper, a modified Von Karman wind spectrum model is used to calculate wind turbine wind field (Bazilevs *et al.* 2011). The model adjusts the error of basic model under the height of 180 m, which is more in line with wind field characteristics of wind turbines. The modified Von Karman wind spectrum is smaller than Davenport and Kaimal wind spectrum in low-frequency region, but on the contrary in the high-frequency region.

$$\frac{fS_{uu}(f)}{\sigma_u^2} = \beta_1 \frac{2.987\dot{n}_u / a}{(1 + (2\pi\dot{n}_u / a)^2)^{5/6}} + \beta_2 \frac{1.294\dot{n}_u / a}{(1 + (\pi\dot{n}_u / a)^2)^{5/6}} F_1 \tag{6}$$

In this formula, S_{uu} is the power spectrum density of stochastic wind speed; f represents the simulated frequency value; σ_u is the standard deviation; $\dot{n}_u$ is the frequency parameter; $\dot{n}_u = fL_{ux}/U_{10}$

with L_{ux} being the integral scale; U_{10} represents the average wind speed at the height of 10 meters; the other calculating parameters are as following

$$F_1 = 1 + 0.455\exp\left[-0.76\left(\frac{\dot{n}_u}{a}\right)^{-0.8}\right] \tag{7}$$

$$\beta_1 = 2.357a - 0.761 \tag{8}$$

$$\beta_2 = 1 - \beta_1 \tag{9}$$

$$a = 0.535 + 2.76\left(0.138 - 0.115\left(1 + 0.315\left(1 - z/h\right)^6\right)^{2/3}\right) \tag{10}$$

where z is the height from the ground, and h is the peripheral layer height.

Because the wind could be considered as Gauss stationary processes, n nodes of wind speed simulation on the wind turbine system are defined, and the stationary Gauss processes with zero mean is assumed. The matrix of the spectral density function is as following

$$S(\omega) = \begin{bmatrix} s_{11}(\omega) & s_{12}(\omega) & \dots & s_{1n}(\omega) \\ s_{21}(\omega) & s_{22}(\omega) & \dots & s_{2n}(\omega) \\ \dots & \dots & \dots & \dots \\ s_{n1}(\omega) & s_{n2}(\omega) & \dots & s_{nn}(\omega) \end{bmatrix} \tag{11}$$

In this formula, $S_{ii}(\omega)$ is auto-power spectrum of the node fluctuating wind, which could be calculated by the wind spectrum model of formula (6); $S_{ij}(\omega)$ is cross-power spectrum. The expression requires the coherence of any two points between the tower and the wind blade or between different towers, and the calculating formula is as following

$$S_{ij}(\omega) = \sqrt{S_{ii}(\omega)S_{jj}(\omega)}C_{ij} \tag{12}$$

The coherence between points on the rotating plane and tower-blade interaction effects should be considered for wind field simulation of wind blade. Then $S(\omega)$ could be obtained by Cholesky decomposition.

$$S(\omega) = H(\omega)\cdot H^*(\omega)^T \tag{13}$$

In this formula $H^*(\omega)^T$ is the conjugate transpose of $H(\omega)$. The three-dimensional matrix of $H(\omega)$ is

$$H(\omega) = \begin{bmatrix} H_{11}(\omega) & 0 & \dots & 0 \\ H_{21}(\omega) & H_{22}(\omega) & \dots & 0 \\ \dots & \dots & \dots & \dots \\ H_{n1}(\omega) & H_{n2}(\omega) & \dots & H_{nn}(\omega) \end{bmatrix} \tag{14}$$

Based on the harmony superposition theory, the time series of fluctuating wind speed of any one node on the tower-blade system can be determined by its power spectrum. The time-history of simulated wind speed can be expressed as

$$v_j(t)=\sum_{m=1}^{j}\sum_{l=1}^{N}\left|H_{jm}(\omega_l)\right|\cdot\sqrt{2\Delta\omega}\cdot\cos\left[\omega_l t+\psi_{jm}(\omega_l)+\theta_{ml}\right]\quad j=1,2,3...n, \tag{15}$$

where the wind spectrum is divided into N equal parts in the frequency range; $\Delta\omega=\omega/N$ represents the increment in frequency; $|H_{jm}(\omega_l)|$ represents the norm of the lower triangular matrix, which is acquired by the Cholesky decomposition of the matrix; θ_{ml} is a random number, which is uniformly distributed between zero and 2π and is generated through the function of Matlab; $\omega_l=l\bullet\Delta\omega$ represents the incremental variable in the frequency domain; $\psi_{jm}(\omega_l)$ represents the phase angle between two different action spots, which is determined by the ratio between the imaginary part of $H_{jm}(\omega_l)$ and the real part of $H_{jm}(\omega_l)$.

$$\psi_{jm}(\omega_l)=\arctan\left(\frac{\mathrm{Im}\left[H_{jm}(\omega_l)\right]}{\mathrm{Re}\left[H_{jm}(\omega_l)\right]}\right) \tag{16}$$

In summary, the time series of fluctuating wind speed for the system can be simulated by formula (15), which considers the coherence effect of any nodes between the wind blades and the tower.

2.3 Aerodynamic loads calculation in yaw condition

The modified blade element momentum theory adopted in this paper introduces the loss of blade root and tip, uses the C_t empirical model when the axial induced factor is bigger, and dynamic inflow and dynamic stall models is also considered. This method could be used to calculate the aerodynamic loads of the wind turbine on different conditions with different wind speed, rotating speed, propeller pitch angle and drift angle.

According to the blade element momentum theory (Wang *et al.* 2012), the relative wind speed V_{rel} on the wind blade can be calculated by the following formula.

$$\begin{pmatrix} v_{rel,x} \\ v_{rel,y} \end{pmatrix}=\begin{pmatrix} v_{ox} \\ v_{oy} \end{pmatrix}+\begin{pmatrix} 0 \\ v_{rot} \end{pmatrix}+\begin{pmatrix} W_x \\ W_y \end{pmatrix}-\begin{pmatrix} v_{bx} \\ v_{by} \end{pmatrix} \tag{17}$$

where V_{ox} and V_{oy} are the flow fluctuating wind speed of downwind and crosswind, respectively, which can be calculated through the harmonic superposition method in the formula (15). v_{rot} represents the linear velocity caused by the rotation of the leaf blades; W represents induced velocity; V_{bx} and V_{by} are the vibrational speeds of the blades. The relationship of all the speed is showed in Fig. 2 (Lanzafame and Messina 2007).

Induced velocity W can be expressed by the following formula (Duquette and Visser 2003)

$$\begin{cases} W_x=\dfrac{-BL\cos\phi}{4\rho\pi rF\left|v_0+f_g n(nW)\right|} \\ W_y=\dfrac{-BL\sin\phi}{4\rho\pi rF\left|v_0+f_g n(nW)\right|} \end{cases} \tag{18}$$

In the formula, B represents the number of blades; L represents the lift force; ϕ represents the upflow angle; ρ represents the density of the air; r represents the span wise location of the section

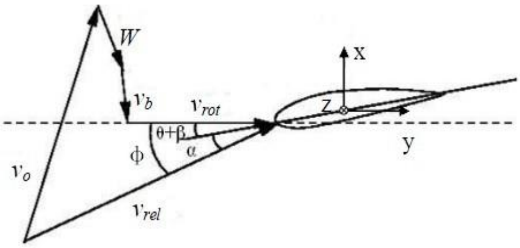

Fig. 2 The local velocity triangle through a wind blade

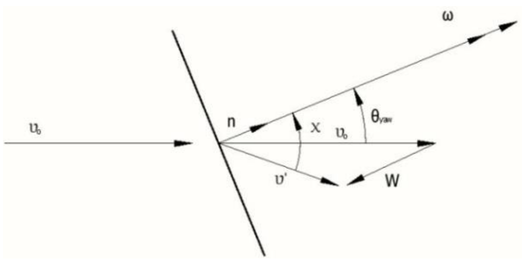

Fig. 3 Schematic diagram of the rotor in yaw condition

of the blade; n represents the single-order vector in the direction of propulsive force; F represents the Prandtl tip loss factor; f_g represents the Glauert correction (Vermeer *et al.* 2003). Meanwhile, the dynamic inflow model and the dynamic stall model are used to correct the unsteady effect of the wind blade.

The induced velocity would generate a slip angle after wind turbine is in a yaw condition (see Fig. 3). The induced velocity of upstream blade is smaller than that of downstream blade, which is caused by that the downstream blade has more area in the wake region, the surface wind velocity is bigger than that of upstream blade. Therefore the aerodynamic loads of downstream blade would be more significant, and the induced velocity calculated by formula (18) should be modified with yaw model by Grau W (Dai and Hu 2011).

$$W = W_o\left[1+\frac{r}{R}\tan\left(\frac{\chi}{2}\right)\cos(\theta_{wing}-\theta_0)\right] \tag{19}$$

where W_0 is the induced velocity calculated by formula (18), θ_0 is the biggest angle of the blade in wake region, x is the skew angle of wake wind speed and blade spindle, which is expressed as follow

$$\cos\chi = \frac{n\cdot v'}{|n|\cdot|v'|} \tag{20}$$

In the formula, n is a normal vector pointing to the rotating axis. Then the angle of attack α of the wind blade is calculated through the following formula

$$\alpha = \phi-(\beta+\theta_{twist}) \tag{21}$$

In the formula, β represents the pitch angle; θ_{twist} represents the geometrical twist angle on the profile of the wind blade, and the calculated formula is

$$\tan\phi = v_{rel,x} / v_{rel,y} \tag{22}$$

The wind turbine airfoil, the lift coefficient C_l and the drag coefficient C_d could be obtained through the interpolation method. Moreover, the lift force L and the resistance D are calculated through the following formula.

$$\begin{cases} L = 0.5\rho\left|v_{rel}\right|^2 C_l c \\ D = 0.5\rho\left|v_{rel}\right|^2 C_d c \end{cases} \tag{23}$$

The normal load F_n and the circumferential load F_t of the wind blade are obtained through the formula.

$$\begin{cases} F_n = L\cos\phi + D\sin\phi \\ F_t = L\sin\phi - D\cos\phi \end{cases} \tag{24}$$

3. Dynamic responses calculation

3.1 Wind turbine tower-blade coupled model

The model was built based on the 5MW wind turbine system with three wind blades, which was developed at Nanjing University of Aeronautics and Astronautics. The tower is 124 m high, of which the bottom has a diameter of 4.8 m and a thickness of 60 mm, while the top has a diameter of 2.6 m and a thickness of 20 mm. Thickness of the tower decreases linearly from the bottom to the top. The nacelle is 12 m long, 4.6 m wide, 4.2 m high, with a total mass of 140.0×10^3 Kg. The wind blade is 60 m long, 2.4 m wide, 0.38 m thick, has a diameter of 120 m, a yaw angle of zero degree and a rated speed of 17.0 r/min.

Traditional wind turbine models mostly suppose perfect rigidity tower, only consider the influence of dynamic blade deformation on aerodynamic loads. In fact, the aerodynamic loads of blades make the deformation of flexible tower more obvious, and the aerodynamic loads and dynamic responses of blades are in turn impacted by tower deformation. Hence, the tower-blade coupled model of wind turbine system was established based on software ANSYS. Both the wind blade and the tower body were simulated by the element of SHELL91; the nacelle and its internal structure were simulated as a whole by the element of BEAM189; the circle raft foundation was simulated by the element of SOLID65. The base is1.8m high and has a diameter of 10 m. It’s assumed that the bottom of the foundation was consolidated, without consideration of the soil-structure interaction. All the components were connected together by the command of multi-element coupling to form an integration model. To reach a compromise between calculating time and calculating precision, the model was divided into 12800 elements. The centrifugal force generated by the rotation of the wind blades was exerted on the wind blades previously as the pre-stressing force during the modal analysis to take into account the effect of centrifugal force (Prowell and Veletzos 2009).

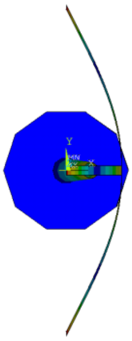

(a) The 1st modal shape

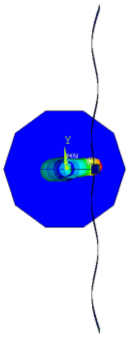

(b) The 20st modal shape

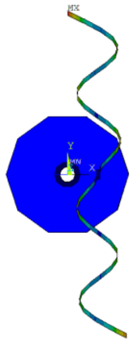

(c) The 50st modal shape

Fig. 4 Typical vibration modes of tower-blade coupled wind turbine model

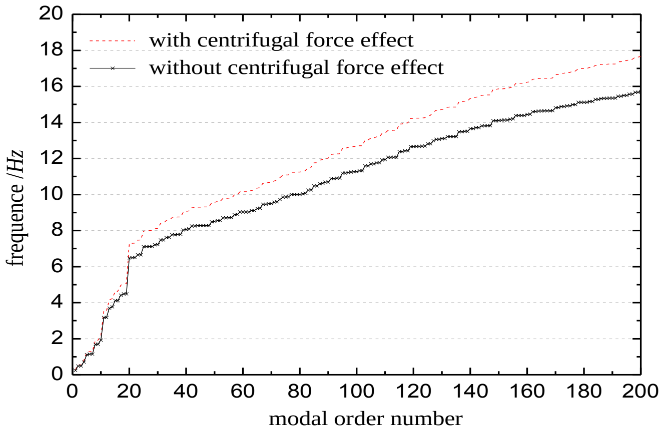

Fig. 5 Scatter gram of natural frequencies in the integration model

According to different modal shapes of the tower-blade system based on the 1st, 20th, and 50th order modes presented in Fig. 4, it is obvious that the vibration modes with lower modal order are mainly in back-forth waving and left-right swinging of the blade, and bending deformation and instability phenomenon in high-order modal appear on the tower, which are coupled with the deformation in back-forth waving and left-right swinging of the blades.

Fig. 5 showed distributions of the first 200 natural frequencies of the tower-blade system considering or ignoring the centrifugal force effect, respectively. It is found that the fundamental frequency of tower-blade system with the centrifugal force effect is slightly larger than that without considering the effect of centrifugal force. Also with the number of modal order increasing, the centrifugal force has a growing influence on the natural frequency. It also shows that the fundamental frequency of the system (0.27 Hz) is very low, the 50th modal frequency is 9.56 Hz, and the interval between modal frequencies is very small.

3.2 Dynamic responses calculation of wind turbine system

The dynamic response of flexible structures to turbulent wind excitation can be expressed in terms of the matrix equations

$$[M]\{\ddot{y}(t)\}+[C]\{\dot{y}(t)\}+[K]\{y(t)\}=\{p(t)\} \tag{25}$$

where $p(t)$ means external stochastic wind load vector; M, C, K mean mass, damping and stiffness matrix, respectively; and $\ddot{y}(t)$, $\dot{y}(t)$ and $y(t)$ are the joint acceleration, velocity and displacement vectors.

Using modal coordinates, Eq. 25 can be expressed as

$$m_i\ddot{q}_i(t)+c_i\dot{q}_i(t)+k_i\ddot{q}_i(t)=P_i(t) \tag{26}$$

where $q_i(t)$=generalized displacement vector of the $i_{\rm th}$ mode, and m_i, c_i, k_i, $p_i(t)$ are generalized modal mass, damping, stiffness, and modal force vector of the $i_{\rm th}$ mode. The numerical solution of dynamic equation of single degree of freedom is as follow according to Duhamel integral principle.

$$\begin{aligned} q_i(t)=\frac{1}{m_i\omega_{di}}\sum_{\tau=0}^{t}p_i(\tau)\exp\left[-\xi_i\omega_{ni}(t-\tau)\right]\bullet \\ \sin\left[\omega_{di}(t-\tau)\right]\Delta\tau,\quad i=1,2,3,\cdots,n \end{aligned} \tag{27}$$

where ω_{ni} is the structural natural mode of vibration, $\omega_{ni}=(k_i/m_i)^{1/2}$, ζ_i is the modal damping ratio, $\zeta_i=b_i/(2m_i\omega_{ni})$, ω_{di} is the structural damping vibration frequency, $\omega_{di}=\omega_{ni}(1-\zeta^2)^{1/2}$, $\Delta\tau$ is the integral time step.

The dynamic displacement response in physical coordinate can be obtained by modal superposition method.

$$\{y(t)\}=\left[\Phi\right]\left\{q(t)\right\} \tag{28}$$

where Φ=matrix of modes of vibration.

The soft ANSYS software is used to calculate wind-induced dynamic responses of wind turbine tower-blade system in time domain, the simulating aerodynamic loads in section 2 are input as external excitation on system. The Newmark-β step-by-step integration method and Newton-Raphson iteration theory are adopted, modal damping ratio is 0.02, integral time step is 0.05s, time step of output responses is 0.025s, intercepting mode number is first 100 orders.

4. Aeroelastic responses calculation method in yaw condition

From the above, the calculating flow of aeroelastic responses for wind turbine tower-blade coupled structure in yaw condition is proposed in Fig. 6. The main calculating procedures are given as follows:

(1) The incoming wind speed considering the modification of steady wind and tower-blade interaction effect is simulated by harmony superposition method, based on the modified Von Karman wind spectra model and Davenport correlation function.

(2) The modified blade element momentum method is used to simulate the induced wind speed of wind turbine tower-blade coupled system considering the wind shear, tower shadow and

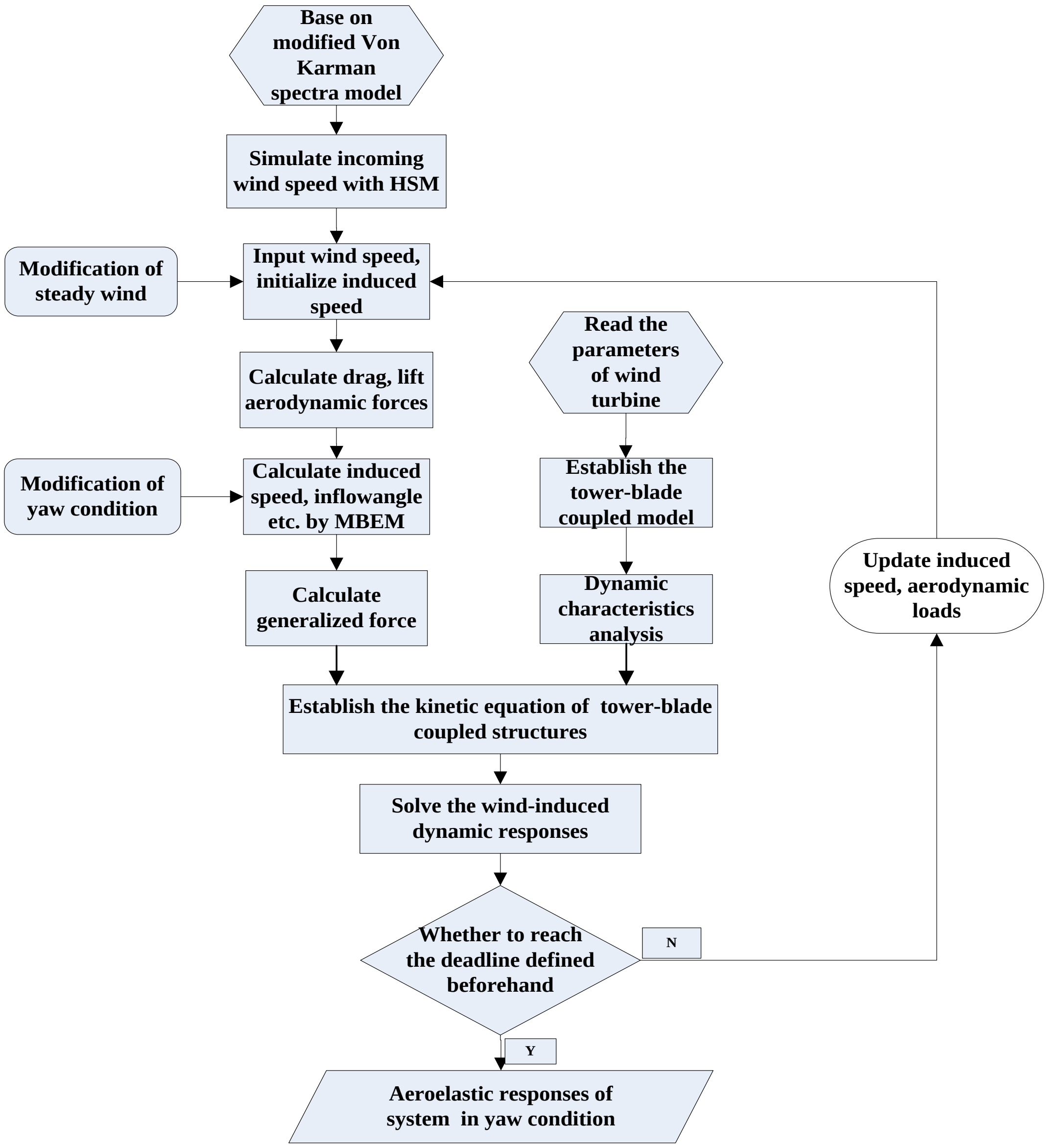

Fig. 6 Flow chart of calculating aeroelastic responses for wind turbines tower-blade system in yaw condition

rotational effects. Then the aerodynamic loads of wind turbine system are obtained through the modification of yaw condition.

(3) The wind turbine tower-blade coupled model is established to solve the dynamic responses under the aerodynamic loads simulated before, then the dynamic responses are returned to update the induced speed and aerodynamic loads. Finally the aeroelastic responses of wind turbine tower-blade coupled model would be obtained by iteration calculation in time domain, until meets the deadline or sample number defined beforehand.

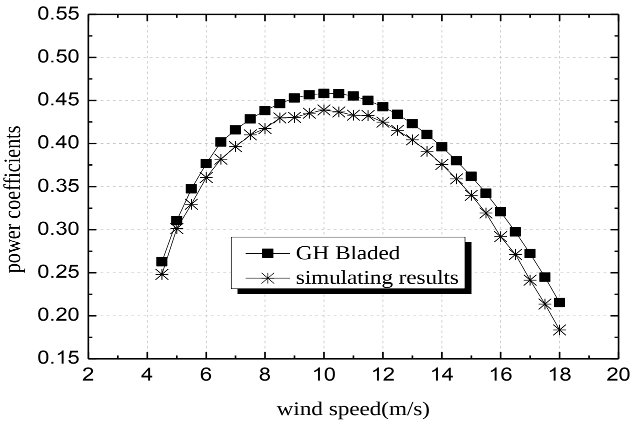

Fig. 7 Power coefficient with different wind speed

5. Example analysis

5.1 Aerodynamic loads and validation

Based on the harmonic superposition method and the modified blade element-momentum theory in this paper, the upper limit frequency of pulsating wind is set to be 2π in the process of calculation. The number of the frequency segmentation points of the fluctuating wind is 2048, and $\Delta\omega$=0.00307 Hz. The average wind speed at the local height of 10m is 24 metres per second. The incoming wind velocity spectrum and coherence function could be obtained via the modified Von Karman wind spectrum model of the formula (5) and the formula (6).

In order to verify the correction of simulation method for wind turbine tower-blade system, the power coefficients of blades is contrasted with the results obtained through professional software GH Bladed (Fig. 7). It is shown from the results that the power coefficients obtained from the present method is slightly smaller than the values obtained through GH Bladed software with the

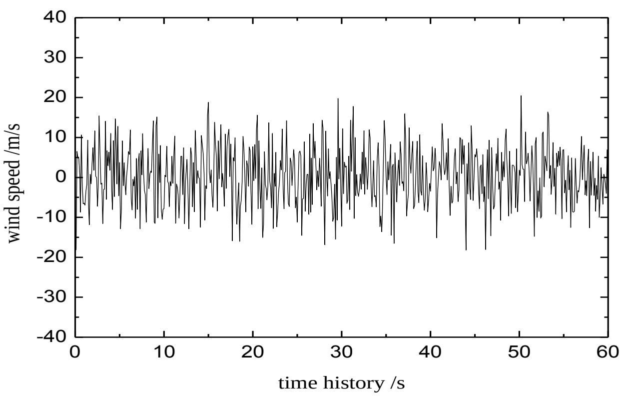

(a) incoming fluctuant wind speed

Fig. 8 Simulating result of fluctuating wind speed of blade

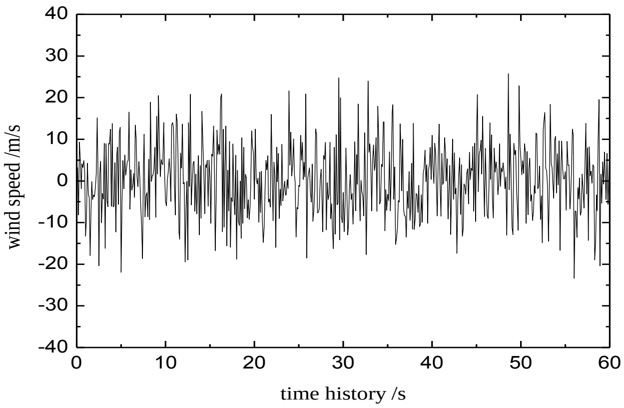

(b) blade fluctuant reference speed

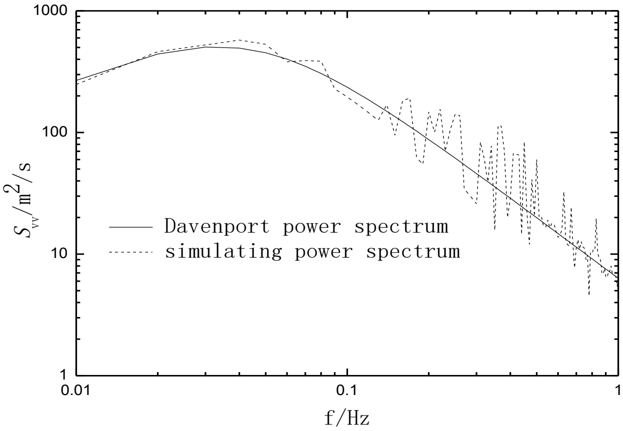

(c) PSD of blade fluctuant wind speed

Fig. 8 Continued

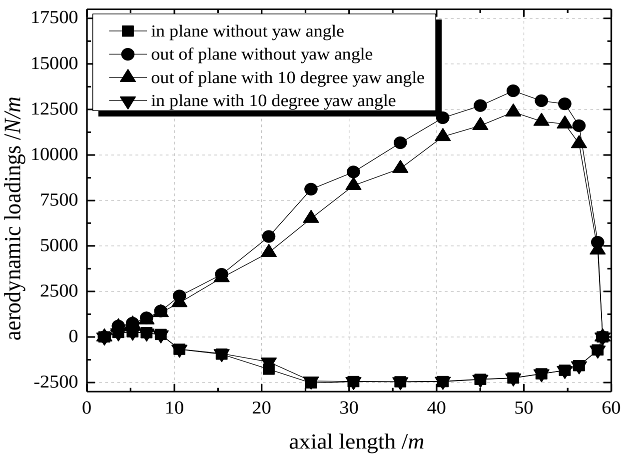

Fig. 9 Distribution curves of aerodynamic loads of blades with or without yaw condition

maximum error is 5% at the wind speed of 11 m/s. This small error is mainly resulted from the wind spectrum model used. The modified Von Karman wind spectrum model is used to simulate the incoming wind field, and the wind energy is smaller than Davenport and Kaimal wind spectrum in low-frequency region, which are adopted in the software GH Bladed. The comparison demonstrates that the simulating method of aerodynamic loads for wind turbine system in this paper is accurate and steady.

The simulating time history and the power spectrum curves of the fluctuating wind speeds on blade are shown in Fig. 8, logarithmic coordinates are adopted in the calculated spectrum of the fluctuating reference wind speed and the Davenport wind spectrum. Fig. 9 shows the aerodynamic load distribution curves of the wind turbine within/without yaw angle inside and outside the plane.

Through the comparative analysis of simulating results, the conclusions are as following:

(1) The wind energy has been increased in reference wind speed compared with incoming fluctuant wind speed, and the wind spectrum presents bigger power amplitude and fluctuant range in high frequencies, which may be caused by tower-blade interaction and rotational effects.

(2) The aerodynamic loads outside plane with yaw angle are obviously smaller than those without yaw angle, nevertheless, the influence of yaw condition on aerodynamic loads inside plane is weak, and the aerodynamic loads inside plane without yaw angle are slightly bigger than those with yaw angle. The aerodynamic loads outside the wind blade plane are much greater than that inside plane, regardless of within the plant or not, the aerodynamic loading increases first and then decreases along the wind blade shaft radius, and the tendency without the plane is more obvious.

5.2 Aeroelastic responses characteristics

Wind turbine system would stop running when the mean wind speed beyond the cut-out wind speed 25 m/s, therefore, the aeroelastic responses of wind turbine tower-blade coupled model with yaw angle 10° under cut-out wind speed are calculated according to the calculating method proposed in Fig. 6. Here Figs. 10 and 11 present the time history curves and power spectral density functions (PSD) of displacement responses for typical parts.

By comparison, the results indicate that the low-frequency resonant effect of blades wind-induced response is very significant, which is caused by that the predominant frequency of

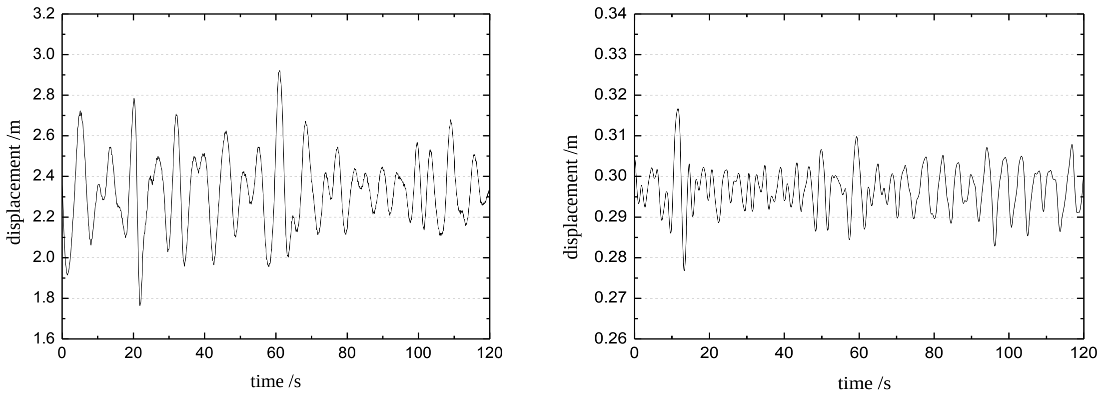

(a) blade tip (b) nacelle

Fig. 10 The displacement time history on typical parts of wind turbine system with yaw angle 10°

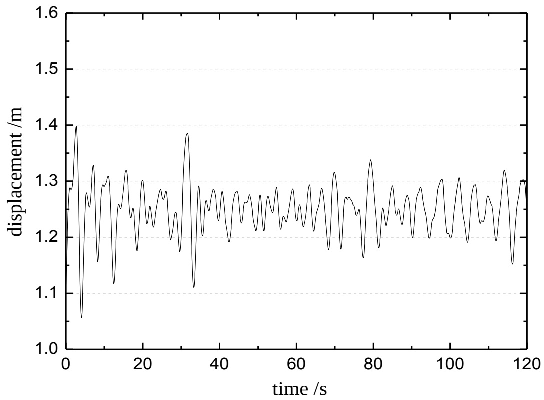

(c) tower top

Fig. 10 Continued

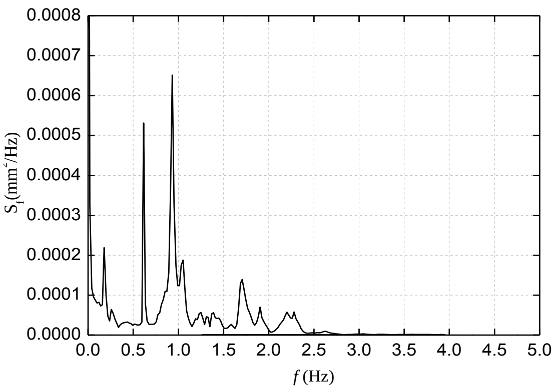

Fig. 11 PSD of displacement on tower top of wind turbine system with yaw angle 10°

wind loads is close to vibration frequency of wind blades. Due to the obvious stiffness of nacelle structure, the dynamic responses mainly present the static or quasi-static characteristics, and the mean response is only 0.295 m. The wind-induced responses of tower top are obviously smaller than that of blade, the contribution of high-order modes is more evident, which is caused by the coupled vibration modes of tower and blades. In general, the aeroelastic responses of wind turbine tower-blade coupled model are characterized with complicated modal responses and multimode coupling effect.

To further investigate the aeroelastic influence on wind-induced responses of wind turbine tower-blade coupled structure, Figs. 12 and 13 show the root mean squares of wind-induced responses with and without aeroelastic effect under different wind speeds. It can been seen that the aeroelastic effect of wind blades would significantly decrease the RMS of dynamic displacement and bending moment responses, especially at the high wind speed, e.g., the maximum error reaches 13.5% at 25 m/s wind speed. At low wind speeds, however, the aeroelastic influence is weak, and the errors are mainly below 5%. Therefore, the aeroelastic effect has obvious influence on wind-induced dynamic responses when wind speed is more than 10 m/s, which should be considered in wind-resistant design of wind turbine system.

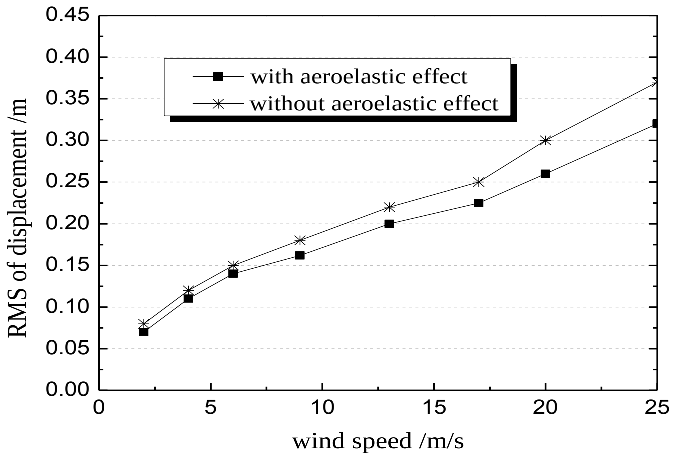

Fig. 12 RMS of along-wind displacement responses of tower top under different wind speeds

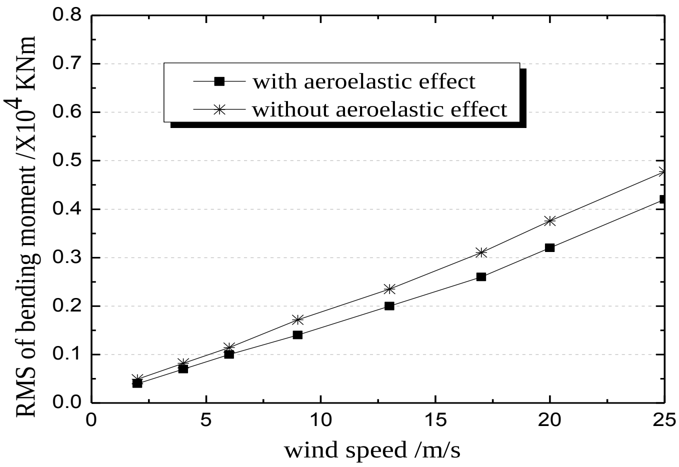

Fig. 13 RMS of bending moment responses of tower bottom under different wind speeds

5.3 impact mechanism of yaw condition

To deeply analyze the impact mechanism of yaw condition on dynamic responses for wind turbine tower-blade coupled structure, the aeroelastic responses of blade tip in back-forth waving direction and right-left swing direction in different yaw angles are provided in Figs. 14 and 15. By comparison the main conclusions are given as follows:

(1) The aeroelastic responses of blade tip in back-forth waving direction and right-left swing direction in different yaw angles are characterized with long-periodic elements, especially with the increase of yaw angle, the aeroelastic responses present more long-periodic characteristics, which also accompanied with the intermittent high magnitude responses.

(2) The impact of yaw angles in back-forth waving direction is very obvious, and with the increase of yaw angle, the fluctuant responses have larger amplitude and smaller mean value. The reason for the phenomenon is that, the increase of yaw angle makes the aerodynamic loads outside

plane progressively smaller, which also leads to the smaller mean value of dynamic response. The induced velocity pointing to downstream will faster access to the wake stream than that pointing to upstream, which results in the much bigger induced velocity pointing to downstream and change of aerodynamic loads, therefore the impact on aeroelastic responses in back-forth waving direction is obvious by change of yaw angles.

(3) The impact of yaw angles in right-left swing direction is weak, and with the change of yaw angle, the fluctuant responses have no obvious variation characteristics. The reason for the phenomenon is that, the aerodynamic and gravitational loads mainly exist in right-left swing direction, the load period is close to rotational period of blades, gravitational load also presents periodical change with blade rotation, so the change of yaw angle has little impact on aeroelastic responses in right-left swing direction.

Table 1 shows the mean, RMS, extreme values of aeroelastic responses for typical objectives with different yaw angles. The analysis results indicate that, the increase of yaw angle would obviously amplify the RMS and reduce the mean response of tower top displacement, the extreme

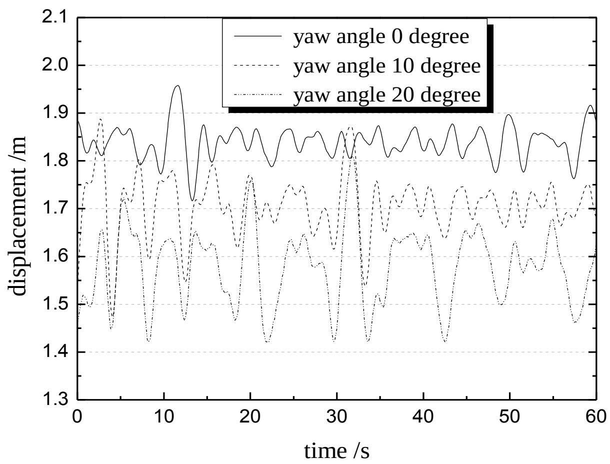

Fig. 14 The aero-dynamic responses in back-forth waving direction under different yaw angles

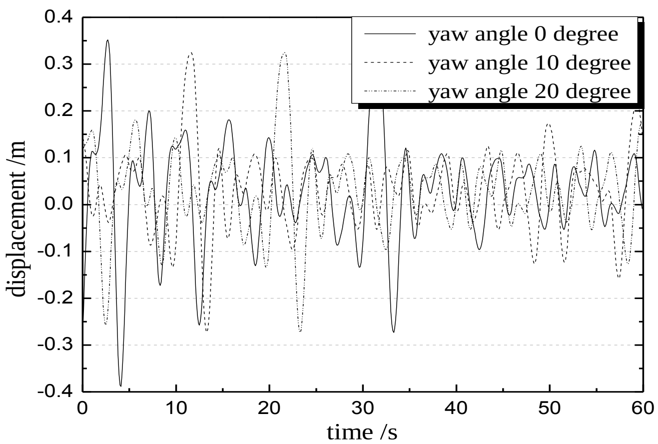

Fig. 15 The aero-dynamic responses in right-left swing direction under different yaw angles

Table 1 The aeroelastic responses of typical objectives under different yaw angles

Yaw angle	Tower top displacement (m)			Tower basis bending moment ($\times 10^3$KN·m)			Balde root shear force ($\times 10^3$KN)		
	mean	RMS	extreme	mean	RMS	extreme	mean	RMS	extreme
0°	0.62	0.24	1.22	3204	512	4484	219	42	324
10°	0.57	0.29	1.295	3085	584	4545	204	51	331
20°	0.53	0.33	1.355	2913	671	4591	197	59	344
30°	0.50	0.39	1.475	2821	729	4644	185	66	350

value response is amplified with the increase of yaw angle. The impact of yaw angles on tower basis bending moment and balde root shear force is not obvious, the impact errors are mostly below 5%, but the change rules are the same with that of tower top displacement.

For a wind rotor in yaw, the aerodynamic loads on the blade are different from azimuth to azimuth, resulting in dynamic responses of the system in different structural multi-frequencies, even in high-order frequencies as shown in Fig.13 in the paper. This is different from the case of axial freestream, where dynamic responses only in low-order frequencies exist due to turbulence wind.

6. Conclusions

In this paper, the aerodynamic loads of large wind turbine tower-blade coupled structure in yaw condition, in which the wind shear, tower shadow, blade-tower dynamic and modal interaction, and rotational effects are taken into account, are simulated based on harmonic superposition method and modified blade element momentum theory. Then based on the mode superposition method in time domain the aeroelastic effect and yaw effect are discussed in detail. The primary conclusions are as follows:

• The simulating method in this paper can accurately calculate the aerodynamic loads of large wind turbine tower-blade coupled structure through the contrast to the results with software GH Bladed. Furthermore, the proposed approach has certain improvement in modification of steady wind and wind spectrum model.

• The yaw effect would obviously amplify the aerodynamic loads outside blades plane, but have weak impact on aerodynamic loads inside blades plane. Furthermore, the fluctuating wind speed spectrum of the wind blades appears energy concentration and larger fluctuation at high frequency.

• The aeroelastic responses of large wind turbine tower-blade coupled structure are characterized with complicated modal responses, multimode coupling effect and multi-loads distribution. The aeroelastic effect would obviously decrease the dynamic responses in the high wind speed, but has weak impact on the dynamic responses in low wind speed.

• The yaw effect is very significant for aeroelastic responses of blade tip in back-forth waving direction, but weak in right-left swing direction, which has been explained from the formation mechanism of aerodynamic loads in this paper. The increase of yaw angle would obviously amplify the RMS and reduce the mean responses, and the extreme value responses are amplified with the increase of yaw angle.

Acknowledgments

The research described in this paper was financially supported by National Basic Research Program of China (2014CB046200), Open foundation for Jiangsu Key Laboratory of Hi-Tech Research for Wind Turbine Design (ZAA1400206) and China Postdoctoral Science Foundation (2015T80551), which are gratefully acknowledged.

References

Agarwal, P. and Manuel, L. (2009), "Simulation of offshore wind turbine response for long-term extreme load prediction", *Eng. Struct.*, **31**(10), 2236-2246.

Barlas, T.K. and Van Kuik, G.A.M. (2009), "Aeroelastic modelling and comparison of advanced active flap control concepts for load reduction on the Upwind 5MW wind turbine", *European Wind Energy Conference*, Marseille, France.

Bazilevs, Y., Hsu, M.C., Kiendl, J., Wüchner, R. and Bletzinger, K.U. (2011), "3D simulation of wind turbine rotors at full scale. Part II: Fluid-structure interaction modeling with composite blades", *Int. J. Numer. Meth. Fluid*., **65**(1), 236-253.

Bazeos, N., Hatzigeorgiou, G.D., Hondros, I.D., Karamaneas, H., Karabalis, D.L. and Beskos, D.E. (2002), "Static, seismic and stability analyses of a prototype wind turbine steel tower", *Eng. Struct*., **24**(8), 1015-1025.

Burton, T., Sharpe, D. and Jenkins, N. (2001), *Wind Energy Handbook*, John Wiley&Sons, Chichester.

Corson, D.A., Griffith, D.T., Ashwill, T. and Shakib, F. (2012), "Investigating Aeroelastic performance of multi-megawatt wind turbine rotors using CFD", *AIAA Structures, 53 rd Structural Dynamics and Materials Conference*, Honolulu.

Dai, J.C., Hu, Y.P., Liu, D.S. and Long, X. (2011), "Aerodynamic loads calculation and analysis for large scale wind turbine based on combining BEM modified theory with dynamic stall model", *Renew. Energy*, **36**(3), 1095-1104.

Davenport, A.G. (1995), "How can we simplify and generalize wind loads?", *J. Wind Eng. Indust. Aerodyn.*, **54**, 657-669.

Duquette, M.M. and Visser, K.D. (2003), "Numerical implications of solidity and blade number on rotor performance of horizontal-axis wind turbines", *J. Sol. Energy Eng.*, **125**(4), 425-432.

Hoogedoorn, E., Jacobs, G.B. and Beyene, A. (2010), "Aero-elastic behavior of a flexible blade for wind turbine application: A 2D computational study", *Energy*, **35**(2), 778-785.

Hsu, M.H. (2008), "Dynamic behaviour of wind turbine blades. Proceedings of the Institution of Mechanical Engineers, Part C", *J. Mech. Eng. Sci.*, **222**(8), 1453-1464.

International Electrotechnical Commission (2006), *Wind Turbine Generator Systems-1: Design Requirements*, International Standard, Geneva.

Jeong, M.S., Kim, S.W., Lee, I., Yoo, S.J. and Park, K.C. (2013), "The impact of yaw error on aeroelastic characteristics of a horizontal axis wind turbine blade", *Renew. Energy*, **60**, 256-268.

Jiménez, Á., Crespo, A. and Migoya, E. (2010), "Application of a LES technique to characterize the wake deflection of a wind turbine in yaw", *Wind Energy*, **13**(6), 559-572.

Kareem, A. (2008), "Numerical simulation of wind effects: a probabilistic perspective", *J. Wind Eng. Indust. Aerodyn.*, **96**(10), 1472-1497.

Karimirad, M. and Moan, T. (2011), "Wave-and wind-induced dynamic response of a spar-type offshore wind turbine", *J. Waterw. Port Coast. Ocean Eng.*, **138**(1), 9-20.

Ke, S.T., Wang, T.G., Ge, Y.J. and Yukio, T. (2014), "Wind-induced responses and equivalent static wind loads of tower-blade coupled large wind turbine system", *Struct. Eng. Mech.*, **52**(3), 485-505.

Lanzafame, R. and Messina, M. (2007), "Fluid dynamics wind turbine design: Critical analysis, optimization and application of BEM theory", *Renew. Energy*, **32**(14), 2291-2305.

Liao, M.F. and Huang, W. (2009), “Fatigue characteristics analysis of wind turbine tower under wind-wave combined effect”, *Acta Energiae Solaris Sinica*, **30**(4), 488-492. (in Chinese)

Lloyd, G. (2005), *GL-2005 rules and guidelines IV-industrial services, part 2-guideline for the certification of offshore wind turbines*, Germanischer Lloyd, Hamburg.

Prowell, I., Veletzos, M., Elgamal, A. and Restrepo, J. (2009), “Experimental and numerical seismic response of a 65 kW wind turbine”, *J. Earthq. Eng.*, **13**(8), 1172-1190.

Tarp, J., Madsen, P.H. and Frandsen, S. (2002), *Partial safety factors in the 3rd edition of IEC 61400 1: wind turbine generator systems-part 1: safety requirements*, Riso National Laboratory.

Shinozuka, M. and Seya, H. (1990), “Stochastic methods in wind engineering”, *J. Wind Eng. Indust. Aerodyn.*, **36**(2), 1472-1497.

Shen, X., Zhu, X. and Du, Z. (2011), “Wind turbine aerodynamics and loads control in wind shear flow”, *Energy*, **36**(3), 1424-1434.

Vermeer, L.J., Sørensen, J.N. and Crespo, A. (2003), “Wind turbine wake aerodynamics”, *Prog. Aerosp. Sci.*, **39**(6), 467-510.

Veers, P.S., Ashwill, T.D., Sutherland, H.J. and *et al.* (2003), “Trends in the design, manufacture and evaluation of wind turbine rotor”, *Wind Energy*, **6**(3), 245-259.

Wang, L., Wang, T.G. and Luo, Y. (2011), “Improved non-dominated sorting genetic algorithm (NSGA)-II in multi-objective optimization studies of wind turbine blades”, *Appl. Math. Mech.*, **32**, 739-748.

Wang, T., Wang, L., Zhong, W., Xu, B. and Chen, L. (2012), “Large-scale wind turbine blade design and aerodynamic analysis”, *Chin. Sci. Bul.*, **57**(5), 466-472.

Zhang, L., Wu, H. and Jing, F.M. (2010), “Study on offshore floating wind turbine and its development”, *Ocean Tech.*, **29**(4), 122-126.

CC